Structure, Volume *20*

Supplemental Information

Tangled Up in Knots: Structures of Inactivated Forms of *E. coli* Class Ia Ribonucleotide Reductase

Christina M. Zimanyi, Nozomi Ando, Edward J. Brignole, Francisco J. Asturias, JoAnne Stubbe, and Catherine L. Drennan

Inventory of Supplemental Information

Figure S1. **Supplement to Figure 3 showing the close-up views and distances that describe some of the key interactions of α_2 and β_2 within the interlocked rings.**

Figure S2. **EM class averages and variance analysis used to generate information shown in Figure 5.**

Figure S3. **Known structures of concatenated proteins for comparison with RNR structures shown in Figure 2.**

Figure S4. **Supplement to Table 1 showing electron density for modeled nucleotides.**

Movie S1 **Movie showing extrapolation between EM images shown in Figure 5B.**

Table S1 **Supplement to Table 1 describing the residues that are modeled in the structures of the two RNR complexes.**

Supplemental Figures

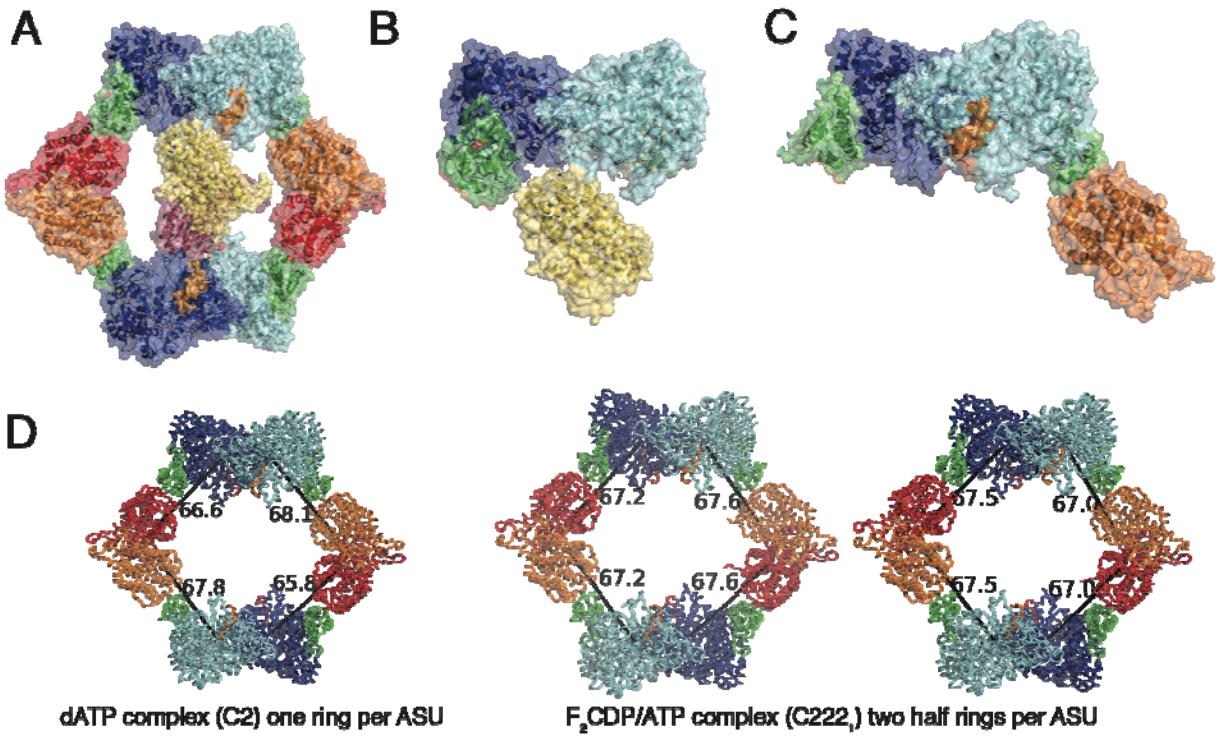

Figure S1. Close-up views and distances describing interactions of α_2 and β_2 within interlocked rings. (**A**) A full ring (α_2 in blue/cyan, β_2 in red/orange, and N-terminal domain of α in green) with the interacting β_2 from a second ring (tan/purple). (**B**) Close-up of interaction between α_2 of full ring and β_2 from second ring. The buried surface area of this interaction is minimal (160 Å^2 in F_2CDP-RNR complex or 400 Å^2 in dATP-RNR complex). (**C**) Close-up of interaction between the α_2 of the full ring (blue/cyan) and its activity site in the N-terminal domain (green) with β of the full ring (orange). This interaction buries 700 Å^2. The C-terminus of this β (orange) is also bound to the peptide-binding site of α (cyan), burying an additional 800 Å^2. (**D**) Asymmetry in the $\alpha_4\beta_4$ ring is seen in the dATP complex. The α_2 dimers are shown in blue/cyan with N-terminal domains in green and the β_2 dimers are shown in red/orange. Distances reported are measured in Å from the C_α of C439 in α to the C_α of Y122 in β for each pair. The structure appears to be rectangle like (two sides measure ~66 Å while the opposing two measure ~68 Å). The F_2CDP complex however is more square-like in structure. The space group symmetry of this crystal form restrains the opposing sides to be of the same length (~ 65 Å). The less symmetrical model (dATP complex) fits better to the previously reported EM structure of the dATP complex (Ando et al., 2011). These differences also highlight a flexibility that is available within the ring structure.

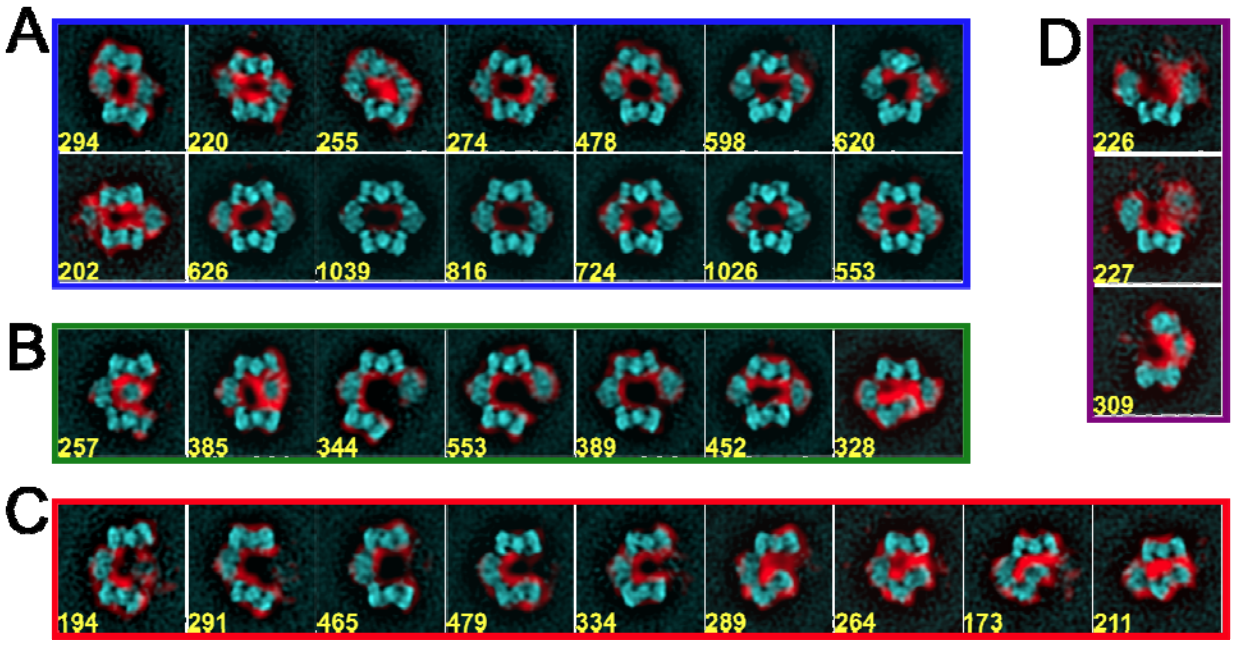

Figure S2. EM class averages and variances reveal malleability of the α-β interaction. Classes are grouped according to subunit stoichiometry and organization into categories of closed $\alpha_4\beta_4$ rings (**A**), opened $\alpha_4\beta_4$ (**B**), $\alpha_4\beta_2$ (**C**), and $\alpha_2\beta_4$ & others (**D**). Boxes around the categories of class averages are colored according to the pie chart in Figure 5C. Class averages (cyan density) were overlaid with the class variances (red density) indicating the presence of additional conformational variation within each class. The number of particles in each class is indicated.

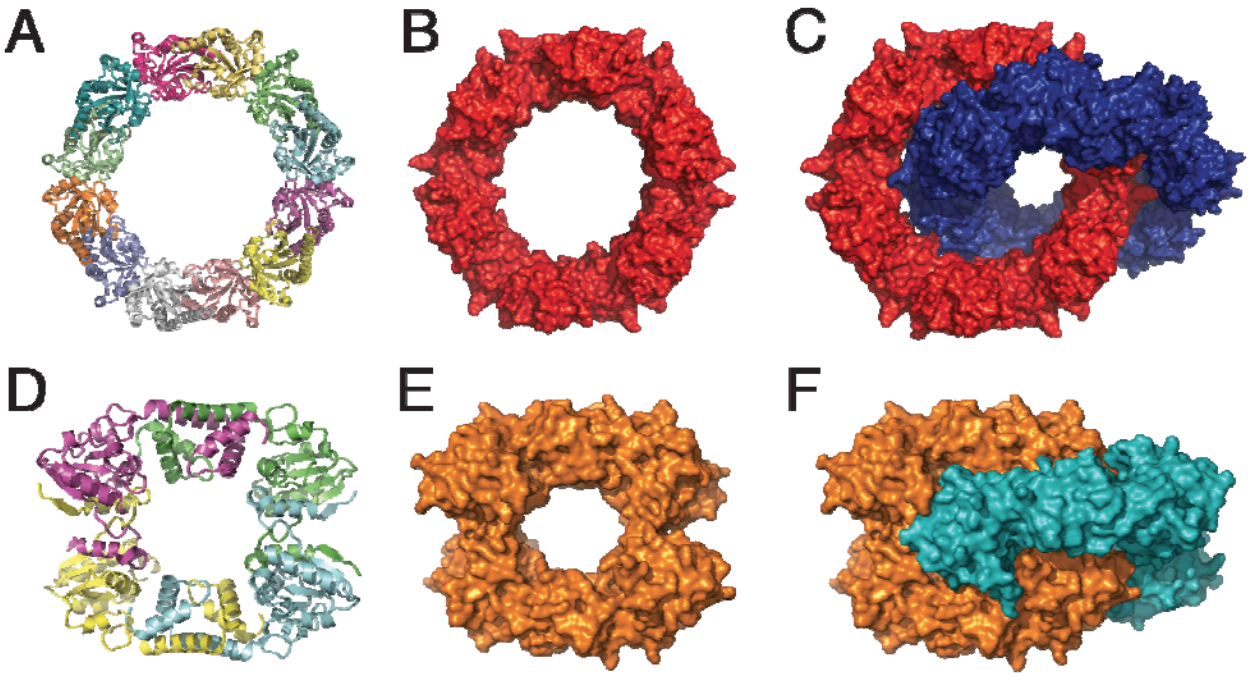

Figure S3. Known structures of concatenated proteins. The crystal structures of (**A**) bovine mitrochondiral peroxiredoxin III (PDB ID 1ZYE) (Cao et al., 2005) and (**D**) the DNA repair protein RecR from *Deinococcus radiodurans* (PDB ID 1VDD) (Lee et al., 2004) contain one ring in the asymmetric unit, shown in ribbons. (**B**) The homododecamer of the peroxiredoxin is shown in surface representation in red. (**E**) The homotetramer or RecR is shown in surface representation in orange. (**C,F**) The ring of a second asymmetric unit (shown in blue or teal) is found to be interlocked with the first in both structures.

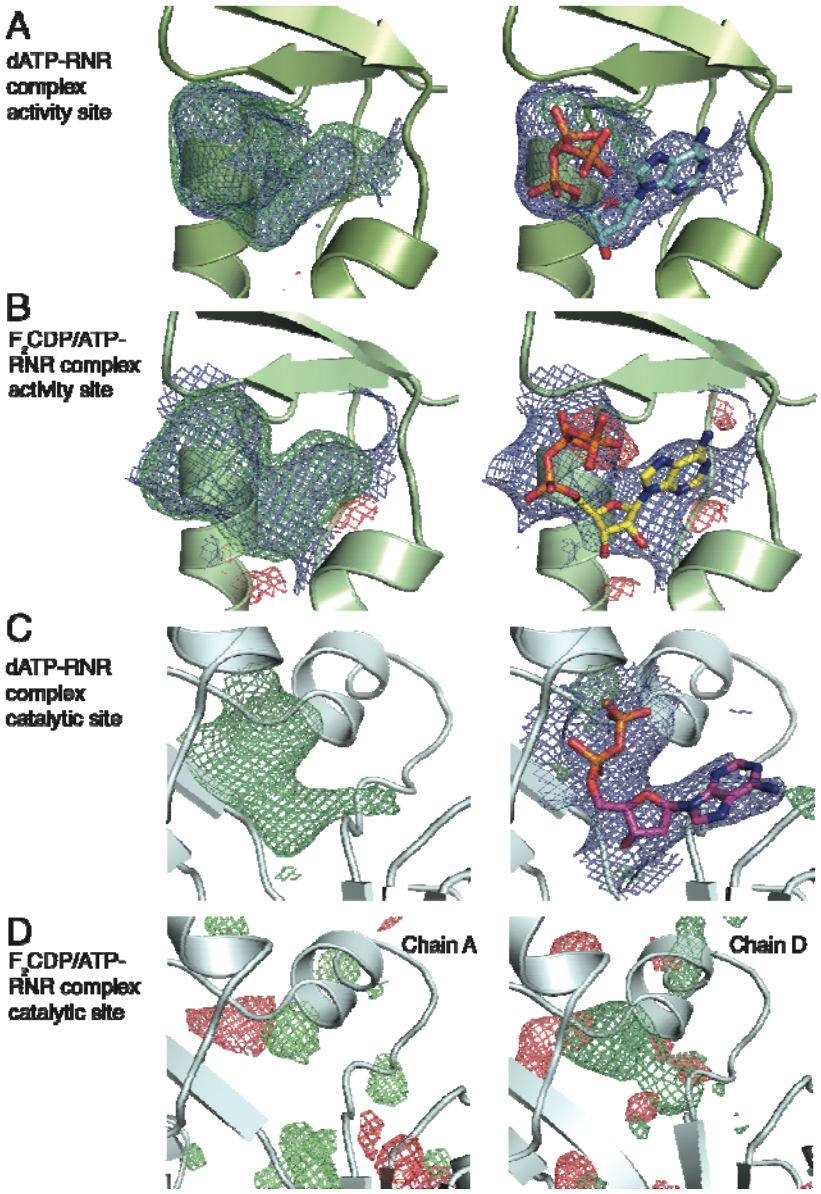

Figure S4. Electron density at activity sites and catalytic sites. In all panels, protein is modeled as ribbons with nucleotides in sticks, (carbon in cyan, yellow, or magenta, oxygen in red, nitrogen in blue, phosphorus in orange). $2F_o$-F_c electron density contoured at 1.0 σ is shown in blue mesh. F_o-F_c electron density contoured at +3.0 σ is shown in green mesh and contoured at -3.0 σ is shown in red mesh. **(A)** Activity site from chain A of the dATP-RNR complex. $2F_o$-F_c and F_o-F_c electron density maps are made with dATP omitted from calculation (left) and included in calculation (right). **(B)** Activity site from chain A of the F_2CDP/ATP-RNR complex shown as in (A) but with ATP modeled. **(C)** Catalytic site from chain A of the dATP-RNR complex with an F_o-F_c electron density difference map made without including the dADP in calculation (left) and $2F_o$-F_c electron density map with modeled dADP (right). **(D)** Catalytic site of the F_2CDP/ATP-RNR complex shown for two chains (chain A on left and chain D on right) with uninterpretable F_o-F_c electron density. $2F_o$-F_c electron density is not shown.

Movie S1. The observed closed and opened $\alpha_4\beta_4$ rings suggest a continuum of conformations hinging on the N-terminal domain. To illustrate this flexibility, trajectories were interpolated between similar conformations (depicted in **Figure 5B**). The coordinates, shown as ribbons, were then assembled into a continuous sequence with grey surfaces simulated by filtering the models to 15 Å resolution.

Table S1. Residues modeled in the structures of the two RNR complexes.

	Chain	Residues modeled
F_2CDP/ATP-RNR complex	Chain A (α)	4-737 (of 761)
	Chain B (α)	4-738
	Chain C (α)	4-736
	Chain D (α)	3-738
	Chain E (β)	1-340, 362-375 (of 375)
	Chain F (β)	1-345, 363-375
	Chain G (β)	1-342, 361-375
	Chain H (β)	1-344, 363-375
dATP-RNR complex	Chain A (α)	4-736 (of 761)
	Chain B (α)	4-737
	Chain C (α)	7-737
	Chain D (α)	5-737
	Chain E (β)	1-339, 363-375 (of 375)
	Chain F (β)	1-340, 360-375
	Chain G (β)	1-340, 360-375
	Chain H (β)	1-341, 360-375